

A Mini-survey of Ultracool Dwarfs at 4.9 GHz

A. Antonova¹, J.G. Doyle¹, G. Hallinan², S. Bourke², A. Golden²

¹ Armagh Observatory, College Hill, Armagh BT61 9DG, N. Ireland

² Computational Astrophysics Laboratory, I.T. Building, National University of Ireland, Galway, Ireland

ABSTRACT

Context. A selection of ultracool dwarfs are known to be radio active, with both gyrosynchrotron emission and the electron cyclotron maser instability being given as likely emission mechanisms.

Aims. To explore whether ultracool dwarfs previously undetected at 8.5 GHz may be detectable at a lower frequency.

Methods. We select a sample of fast rotating ultracool dwarfs with no detectable radio activity at 8.5 GHz, observing each of them at 4.9 GHz.

Results. From the 8 dwarfs in our sample, we detect emission from 2MASS J07464256+2000321, with a mean flux level of $286 \pm 24 \mu\text{Jy}$. The light-curve of 2MASS J07464256+2000321, is dominated towards the end of the observation by a very bright, $\approx 100\%$ left circularly polarized burst during which the flux reached 2.4 mJy. The burst was preceded by a raise in the level of activity, with the average flux being $\approx 160 \mu\text{Jy}$ in the first hour of observation rising to $\approx 400 \mu\text{Jy}$ in the 40 minutes before the burst. During both periods, there is significant variability.

Conclusions. The detection of 100% circular polarization in the emission at 4.9 GHz points towards the electron cyclotron maser as the emission mechanism. However, the observations at 4.9 GHz and 8.5 GHz were not simultaneous, thus the actual fraction of dwarfs capable of producing radio emission, as well as the fraction of those that show periodic pulsations is still unclear, as indeed are the relative roles played by the electron cyclotron maser instability versus gyrosynchrotron emission, therefore we cannot assert if the previous non-detection at 8.5 GHz was due to a cut-off in emission between 4.9 and 8.4 GHz, or due to long term variability.

Key words. Stars: low-mass, brown dwarf – Radio continuum: stars – Radiation mechanism: general – Masers

1. Introduction

Ultracool dwarfs (UCDs) are defined as those dwarfs with spectral type M7 or later (Kirkpatrick et al. 1997). Due to the low and in most instances non-detectable levels of $H\alpha$ and X-ray emission, radio emission was considered to be insignificant until Berger et al. (2001) reported a detection from the brown dwarf LP 944-20. Additional sources were reported by Berger (2002), Burgasser & Putman (2005), Berger (2006) and Phan-Bao et al. (2007) with the emission mechanism assumed to be gyrosynchrotron. A highly polarized flare, detected by Burgasser & Putman (2005) from the M8 dwarf DENIS 1048-3956, was interpreted as due to coherent electron cyclotron maser emission.

Hallinan et al. (2006) reported a periodicity in the radio emission of the UCD TVLM 513-46546 (hereafter TVLM 513), consistent with the rotation period of the dwarf (Lane et al. 2007). They suggested that the emission process was due to an electron cyclotron maser (ECM), similar to the emission process in the magnetized planets in the solar system (Zarka 1998, Ergun et al. 2000). In a higher sensitivity followup study, Hallinan et al. (2007) observed extremely bright, periodic bursts of both left and right hand 100% circularly polarized emission from the same source. The characteristics of these short duration bursts were consistent with a coherent process, the electron cyclotron maser instability.

There have been a number of surveys of ultracool dwarfs in the radio (see references above). Thus far, 9 out of the ≈ 100 UCDs observed at radio frequencies have been detected as radio sources. All of these surveys, however, were conducted at 8.5 GHz. This may have major implications for the number of

radio active cool dwarfs if the electron cyclotron maser is the dominant mechanism as in this case the emission is mostly at the fundamental or second harmonic of the cyclotron frequency $\nu_c \approx 2.8 \times 10^6 \text{B}[\text{Hz}]$, i.e. for an object to have detectable emission at 8.5 GHz requires a magnetic field strength of ≈ 3 kG. Thus, it is possible that dwarfs, with maximum field strengths below that value may be detectable in the radio at lower frequencies.

In order to investigate this possibility, we conducted observations with the Very Large Array (VLA)¹ for a sample of 8 ultracool dwarfs (previously undetected at 8.5 GHz) at the lower frequency of 4.9 GHz. Here we present the results of our observations and the detection of another ultracool dwarf producing electron cyclotron maser emission, the L0.5 binary system 2MASS J07464256+2000321.

2. The Sample

Our sample consists of 8 ultracool dwarfs spanning the spectral range M8.5 – T6. All our targets were previously undetected at 8.5 GHz. Below we summarize the main properties of each dwarf in the sample.

2MASS J03350208+2342356 (2MASS0335+23)

This object was identified as a young M8.5 brown dwarf, based on the presence of Li I absorption, situated at a distance of ≈ 19.2 pc (Gizis et al. 2000, Reid et al. 2002). It also exhibits $H\alpha$ emission, with $EW_{H\alpha}$ in the range 4.6 – 6.5Å, while Berger

¹ The National Radio Astronomy Observatory is a facility of the National Science Foundation operated under cooperative agreement by Associated Universities, Inc.

(2006) reported an 8.5 GHz radio emission upper limit of $< 69 \mu\text{Jy}$. The projected rotational velocity $v \sin i = 30 \text{ km s}^{-1}$ (Reid et al. 2002).

2MASP J0345432+254023 (2MASS0345+25)

This is an L0 spectral type brown dwarf (Kirkpatrick et al. 1999) with $v \sin i \approx 25 \text{ km s}^{-1}$ (Berger, 2006 and references therein). It shows no evidence of H α or Li I emission, has $T_{\text{eff}} \approx 2430 \text{ K}$, $\log(L_{\text{bol}}/L_{\odot}) = -3.58 \pm 0.06$ (Vrba et al. 2004) at an estimated distance of 27 pc (Gizis et al. 2003). Bailer-Jones & Mundt (2001) reported it as photometrically variable. The upper limit for the 8.5 GHz radio flux, given by Berger (2002) is $< 88 \mu\text{Jy}$.

2MASS J07464256+2000321 (2MASS0746+20)

This dwarf was discovered by Kirkpatrick et al. (2000) and was later resolved as a near equal mass binary system, with a separation of 2.7 AU (Reid et al. 2001). Dahn et al. (2002) determined its distance to be $12.2 \pm 0.05 \text{ pc}$. Vrba et al. (2004) estimated $\log(L_{\text{bol}}/L_{\odot}) = -3.64$ for the system, with an effective temperature in the range $1900 < T_{\text{eff}} < 2225 \text{ K}$. Several studies reported detection of H α emission and only an upper limit on Li I (Bouy et al. 2004). In the radio, Berger (2006) give an upper limit of $F_{8.5\text{GHz}} < 48 \mu\text{Jy}$. Bouy et al. (2004) made the first measurement of the dynamical mass of the system, classifying both components as $L0 \pm 0.5$ and $L1.5 \pm 0.5$ respectively. In a recent study, Gizis & Reid (2006) argued that it is still unclear whether 2MASS0746+20B is actually a brown dwarf. They argue that the system is much older ($\geq 1 \text{ Gyr}$) and the second component has a mass which is above or just at the sub-stellar limit. Rotational velocity studies give $v \sin i$ in the range $23.0 - 28.8 \text{ km s}^{-1}$ and a rotational period between 1.84 and 5.28 hrs (Bailer-Jones, 2004). Such a rotational period is in very good agreement with a photometric variability detected by Clarke et al. (2002), with a periodicity of $\approx 3 \text{ hrs}$.

2MASS J22244381-0158521 (2MASS2224-01)

This is another fast rotator, e.g. Bailer-Jones (2004) reported a projected rotational velocity in the range $20.9 < v \sin i < 29.2 \text{ km s}^{-1}$ giving an expected rotational period of 3.8 hrs. The dwarf was first discovered by Kirkpatrick et al. (2000), classifying it as L4.5. The distance to the dwarf is 11.4 pc, it has $T_{\text{eff}} \approx 1790 \text{ K}$ (Dahn et al. 2002) and a bolometric luminosity $\log(L_{\text{bol}}/L_{\odot}) = -4.15 \pm 0.02$ (Golimowski et al. 2004). H α emission has been detected, with $EW_{\text{H}\alpha} = 1 \text{ \AA}$ and only an upper limit for Li I (Kirkpatrick et al. 2000). In the radio, Berger (2006) gives an upper limit of the flux at 8.5 GHz $< 33 \mu\text{Jy}$.

2MASS J15074769-1627386 (2MASS1507-16)

This is a nearby L5 brown dwarf, located at 7.3 pc (Dahn et al. 2002). It has an estimated age of $\geq 1 \text{ Gyr}$ and $T_{\text{eff}} \approx 1700 \text{ K}$, $\log(L_{\text{bol}}/L_{\odot}) = -4.27 \pm 0.05$ (Vrba et al. 2004) and only upper limits on Li I and H α of less than 0.1 \AA and 0.5 \AA respectively (Reid et al. 2000). For this dwarf, Bailer-Jones (2004) reported a projected rotational velocity of $v \sin i \approx 27 \text{ km s}^{-1}$ giving an expected rotational period of 3.5 hrs. Berger (2002) give an upper limit to the 8.5 GHz radio flux as $< 36 \mu\text{Jy}$.

2MASS J13054019-2541059 (Kelu-1)

This is the fastest rotator in our sample with $v \sin i = 60 \pm 2 \text{ km s}^{-1}$ (Mohanty & Basri 2003), it has a parallax of 18.7 pc (Dahn et al. 2002), and a bolometric luminosity of $\log(L_{\text{bol}}/L_{\odot}) = -3.59 \pm 0.04$, which together with an age, constrained to 0.3 - 1 Gyr, yields $T_{\text{eff}} = 2100 - 2350 \text{ K}$

(Golimowski et al. 2004 and references therein). Kelu-1 appears over-luminous compared to other early type L dwarfs, which could be either due to a very young age or a close companion (Leggett et al. 2002). It exhibits H α emission (Ruiz et al. 1997) but is undetected in X-rays (Neuhäuser et al. 1999) and radio wavelengths. Berger (2006) gives an upper limit of $< 27 \mu\text{Jy}$ at 8.5 GHz. Using the Keck laser guide star adaptive optics system, Liu & Leggett (2005) resolved the dwarf as a binary with separation 5.4 AU, with estimated spectral types L1 - L3 and L3 - L4.5 respectively, with masses in the sub-stellar regime for both components. Recently Audard et al. (2007) conducted simultaneous X-ray and 8.5 GHz observations of this system, resulting in a detection in X-rays, $L_X = 2.9 \times 10^{25} \text{ erg s}^{-1}$ and a 3σ upper limit of $42 \mu\text{Jy}$ at 8.5 GHz.

SDSS J162414.37+002915.6 (SDSS1624+00)

This is the first field T dwarf discovered (Strauss et al. 1999), and is classified as a T6. It has a parallax of $11.00 \pm 0.15 \text{ pc}$ (Burgasser et al. 2006) and a bolometric luminosity $\log(L_{\text{bol}}/L_{\odot}) = -5.16 \pm 0.05$. It has a rotational velocity of $v \sin i = 34 - 38 \text{ km s}^{-1}$ (Zapatero Osorio et al. 2006). It has no detected H α emission (Burgasser et al. 2000) and no detection of radio emission at 8.5 GHz ($F_{8.5\text{GHz}} < 36 \mu\text{Jy}$, Berger 2006).

2MASP J1632291+190441 (2MASS1632+19)

This is an L8 brown dwarf, first discovered by Kirkpatrick et al. (1999), situated at a distance of 15.2 pc (Dahn et al. 2002). It's effective temperature and luminosity are $T_{\text{eff}} = 1346 \text{ K}$ and $\log(L/L_{\odot}) = -4.6$ respectively (Vrba et al. 2004). This dwarf has upper limits for emission in both H α (Mohanty & Basri 2003) and radio ($F_{8.5\text{GHz}} < 36 \mu\text{Jy}$, Berger 2006). The reported projected rotational velocity for 2MASS1632+19 is $v \sin i = 30 \pm 10 \text{ km s}^{-1}$ according to Mohanty & Basri (2003), while Zapatero Osorio et al. (2006) give $20.9 \pm 7.0 < v \sin i < 22.6 \pm 6.7 \text{ km s}^{-1}$.

3. Observations and Data Reduction

The observations were conducted at a frequency of 4.9 GHz (6 cm) with the NRAO Very Large Array (VLA) on 22–23 January 2007. During the observations, the instrument was in full array mode and DnC configuration. We used the standard continuum mode with 2×50 contiguous bands, sampling every 10 s. The flux density calibrator was 3C147. The phase was monitored using calibration sources selected to be within 10 degrees of the target. The total time on each source was 2 hours (time on source in a single scan being 8 minutes, before moving to the phase calibrator for 90 s) enabling 3σ confirmation of all sources with average flux levels of $> 60 \mu\text{Jy}$.

Data reduction was carried out with the Astronomical Image Processing System (AIPS) software package. The visibility data were inspected for quality both before and after the standard calibration procedures, and noisy points removed. For imaging the data, we used the task IMAGR. We also CLEANed the region around each source and used the UVSUB routine to subtract the resulting source models for the background sources from the visibility data. We then used the task UVFIX to shift the tangent point coordinates of the target source to coincide with the phase centre of the map. The subtraction of the background sources and the shifting of the map are necessary since the side-lobes of those sources and the change in the synthesised beam shape during the observation may result in creating false variability of the target source, or contamination of any real variability present. As a next step we re-imaged the visibility data set in both to-

Table 1. The sample of 8 ultracool dwarfs.

Name	α (J2000)	δ (J2000)	SpT	π (mas)	$v \sin i$ (km s ⁻¹)	$F_{(4.9 \text{ GHz})}$ (μJy)
2MASS 0335+23	03 35 02.08	+23 42 35.6	M8.5	51.2	30	< 45
2MASS 0345+25	03 45 43.16	+25 40 23.3	L0	37.1	25	< 36
2MASS 0746+20	07 46 42.56	+20 00 32.2	L0.5	81.9	25.8	286 \pm 24
Kelu-1	13 05 40.18	-25 41 06.0	L2	53.6	60.0	< 84
2MASS 1507-16	15 07 47.69	-16 27 38.6	L5	136.4	27.2	< 57
SDSS 1624+00	16 24 14.37	+00 29 15.6	T6	91.5	36	< 81
2MASS 1632+19	16 32 29.11	+19 04 40.7	L8	65.6	30.0	< 39
2MASS 2224-01	22 24 43.81	-01 58 52.1	L4.5	88.1	24.7	< 46

Note. - The columns are (left to right): name of the object; right ascension; declination; spectral type; parallax; rotational velocity; radio flux at 4.9 GHz. References. Ruiz et al. (1997), Kirkpatrick et al. (1999), Strauss et al. (1999), Gizis et al. (2000), Kirkpatrick et al. (2000), Berger (2002), Dahn et al. (2002), Reid et al. (2002), Gizis et al. (2003), Mohanty & Basri (2003), Bailer-Jones (2004), Golimowski et al. (2004), Vrba et al. (2004), Berger (2006), Zapatero Osorio (2006).

tal intensity (Stokes I), and circular polarization (Stokes V). For examining the light curves we used the AIPS task DFTPL.

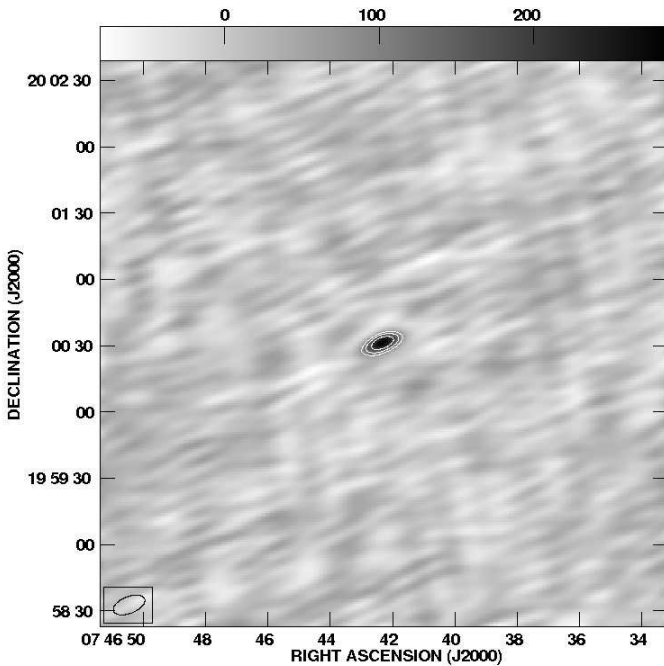


Fig. 1. A VLA map of 2MASS0746+20 at 4.9 GHz with the background sources removed. The image is in total intensity (Stokes I). Over-plotted are the 3, 5 and 8 σ contour levels, where 1 σ = 24 μJy . The beam size is shown at the bottom left corner of the map.

4. Results

In Table 1 we list the main properties of the observed sources, as well as the measured radio flux or upper limits at 4.9 GHz, based on detection/non-detection respectively. From the 8 dwarfs in our sample, we detect emission from 2MASS0746+20, with a mean flux level of 286 \pm 24 μJy (Fig. 1). The object's derived position was consistent with its expected location after correcting for proper motion (Dahn et al. 2002).

The flux, detected from 2MASS0746+20 implies a radio luminosity $L_{4.9\text{GHz}} = 5.09 \times 10^{13} \text{ erg s}^{-1} \text{ Hz}^{-1}$ and $\log(L_{R,\nu}/L_{bol}) = -16.24$. Due to the low spatial resolution of our observation,

we do not resolve the system, thus we cannot determine which component is dominant.

To further examine the behaviour of the source, we plot its light-curve in total intensity (Stokes I) and circular polarization (Stokes V) (Fig. 2). We show three different time resolutions (10s, 30 s and 180 s) The light-curve of 2MASS0746+20, is dominated towards the end of the observation by a very bright, $\approx 100\%$ left circularly polarized burst during which the flux level reached 2.3 mJy. The burst was preceded by a raise in the level of activity, with an average flux of $\approx 160 \mu\text{Jy}$ in the first hour of observation rising to $\approx 400 \mu\text{Jy}$ in the 40 minutes before the burst. This rise is in part due to a series of other bursts, e.g. one at 4.3 hr. and another at 4.6 hr. Unfortunately, the larger of these occurs during a phase calibration, and thus we only detect the rise and delay. It is however detectable in both I and V.

The above fluxes were determined by separately imaging the two time intervals. During both intervals, there is significant variability. Because the total observing time (2 hours) is less than the expected rotational period of the dwarf (~ 3.7 hours, Bailer-Jones 2004), searching for rotational modulation (as in Hallinan et al. 2006, 2007) is not possible.

As a next step, we imaged the field around the dwarf separately in three time intervals in both Stokes I and Stokes V, keeping a close-by (~ 12 arcsec), bright background source for comparison. Fig. 3 shows the resulting maps. The top left panel shows the Stokes I map of the 3 to 4 hrs UT interval, the top right panel is the Stokes I map during the 4 – 4.75 hrs UT interval, while the bottom left and right show Stokes I and Stokes V images of the last 10 minutes of the observation. The background source is the dominant feature in the map during the first two intervals (as well as the map of the entire 2 hour observation), while in the last one, it is actually fainter than 2MASS 0746+20 in total intensity and is absent from the map in circular polarization, where the ultracool dwarf is clearly visible. Imaging the map in Stokes V during the first two time intervals did not reveal a source at the position of the dwarf.

The behaviour of the 2MASS0746+20 light-curve, i.e. the low flux levels at the start of the observation, followed by a brightening and a strong, but short-lived burst, led us to an interesting question. What if a source has pulsed emission, but its quiescent emission is absent, or too low to be detected? In this case, since the pulses span only a few minutes, the overall flux will be very low and most likely at, or below the 3 σ detection limit. If $F_p/F_q > \sqrt{t_q/t_p}$, where F_p and F_q are the flux density during a pulse and the average flux density of the whole observation, and t_p and t_q are the duration of the pulse and the duration of the whole observation respectively, the SNR will be

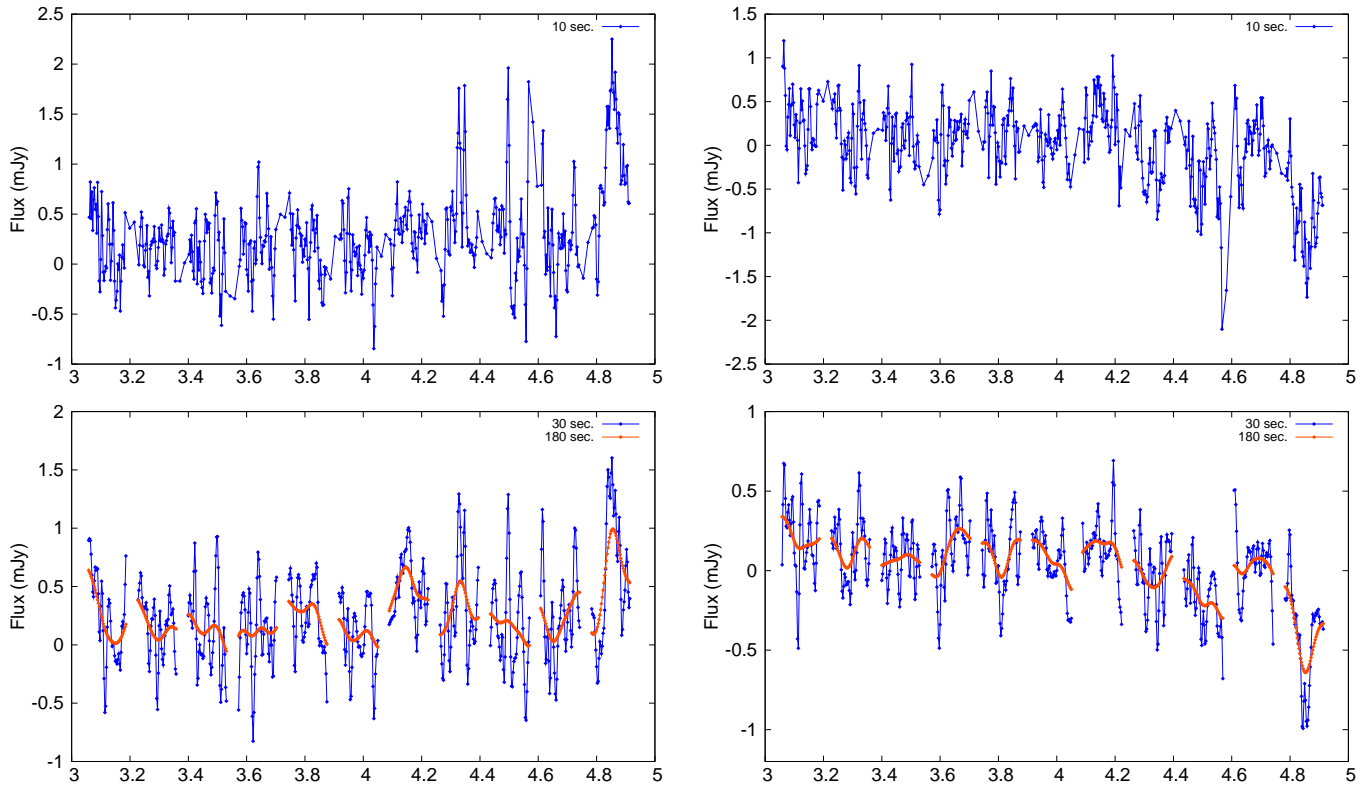


Fig. 2. The light curves of the total intensity (Stokes I) (left) and circular polarization (Stokes V) (right) radio emission, detected at 4.9 GHz from 2MASS0746+20. The data, taken with the VLA in January 2007, is smoothed over 10s (top panels) and 30 s & 180 s (bottom panels) time intervals. The gaps in the data in the bottom panels of the figure are due to phase calibration. In the Stokes V light curve, right circular polarization is represented by positive values, while left circular polarization is represented by negative values. A 100 % left circularly polarized burst is evident in the last 10 minutes of the observation.

higher for the pulse than for the entire observation. To investigate such a possibility, we reexamined our X band data for TVLM 513 (Hallinan et al. 2007), taken with the VLA in May 2006. It spans over 10 hours, covers 5 periods of rotation of the dwarf and clearly shows bursts of 100% left and right circularly polarized flux. The SNR of a single 8 min burst exceeded the SNR of the entire observation by factor of 1.5 (for 2MASS0746+20 the SNR during the pulse exceeds the SNR of the whole observation by a factor of 2). Therefore to rigorously determine whether an ultracool dwarf is detected or not, it is necessary to image subsets of the data for the possible presence of pulses.

To determine which subsets to image, we produced three sets of ten second resolution time series of the May 2006 TVLM 513 data: with the source at the phase center and the field sources removed, with the source at the phase center and the field sources still present and a set of time series with the source not at the phase center but with the field sources present. Comparing those three sets of time series, showed that even though the presence of the background sources affects the shape of the target’s light-curve, the pulses are still clearly visible when the target is at the phase centre of the map. If the target is shifted from the phase centre, the shape of the light-curve changes drastically and the pulses are no longer visible. We repeated the same experiment on our 2MASS0746+20 data. The result was the same - even with the background sources present, when the dwarf is at the phase centre, i.e. the burst in the last 10 min of the observation is still clearly present in the light curve. Shifting the position of

the target off, on the other hand, makes the picture less clear and the presence of the burst is not obvious.

Encouraged by these results, we repeated the experiment for the rest of the targets in our sample. We first acquired from the literature accurate proper motion measurements for each dwarf, then calculated the dwarfs’ coordinates at the epoch of our observation. Using the AIPS task UVFIX, we shifted the phase centre of every map to coincide with the position of the respective dwarf and then plotted the visibilities in both total intensity and circular polarization, using the task DFTPL. Inspecting the light curves did not reveal any additional detections.

5. Discussion

Until recently, radio emission from UCDs has been attributed to incoherent gyrosynchrotron emission, similar to that detected from early to mid-type M dwarfs (Berger et al. 2005, 2006, Burgasser & Putman 2005, Osten et al. 2006). However, Hallinan et al. (2006) argued that the more likely scenario is a coherent, electron cyclotron maser emission from a low-density region above the magnetic poles of the dwarf. This model would require the presence of a stable, large-scale magnetic field, with field strengths ≈ 3 kG. The presence of fields with such strength on low mass stars and UCDs has been suggested by direct observations (Donati et al. 2007 and Reiners & Basri 2007). Subsequent observations of TVLM 513 (Hallinan et al. 2007) have revealed extremely bright, periodic, 100% circularly polarized bursts, produced by the strong beaming of the radio emis-

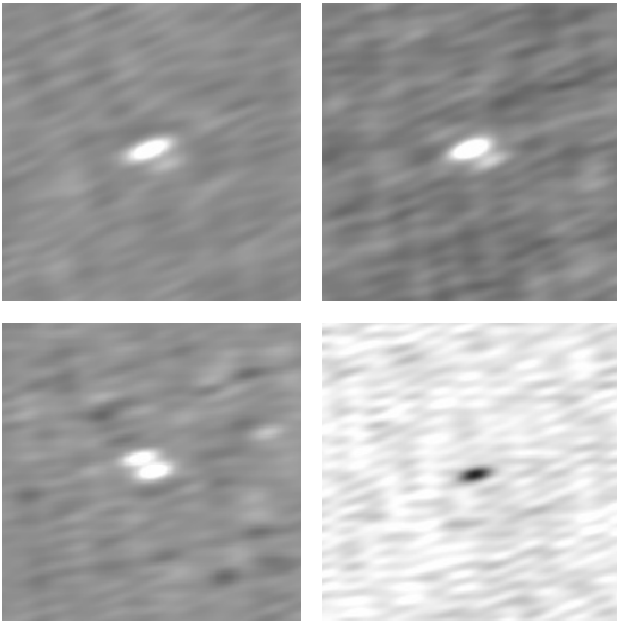


Fig. 3. Field maps of the binary dwarf 2MASS0746+20. Top left - Total intensity (Stokes I) image of the first one hour of observation (3 – 4 hours UT). The dwarf’s position is to the lower right of the bright field source. Top right - Stokes I image of the 4 – 4.75 hours UT interval, when the flux level of 2MASS0746+20 is found to be rising. Bottom left - Stokes I image of the last 10 minutes of the observation. The dwarf is brighter than the background source during this heightened period of emission. Bottom right - Stokes V image of the last 10 minutes of the observation. 2MASS0746+20 is a source of highly circularly polarized emission, while the background source is completely absent from the map.

sion and the rapid rotation of the dwarf. These properties, especially the high levels of polarization and the inherent directivity of the emission, together with the resulting high brightness temperature, provide confirmation of the coherent nature of the emission.

For the electron cyclotron maser operation, a population inversion in the electron distribution is needed, as well as a relatively strong magnetic field and low-density plasma, so that the electron cyclotron frequency ν_c is greater than the plasma frequency ν_p , where $\nu_c \approx 2.8 \times 10^6 B [\text{Hz}]$ and $\nu_p \approx 9000 n_e^{1/2} \text{ Hz}$. An efficient mechanism for reaching the necessary anisotropy in the electron distribution, is the shell instability, proposed as a source of Earth’s auroral kilometric radiation, when it became clear that the loss-cone distribution was a poor fit to the observations (see Treumann 2006 for review). It is suggested that the main source for any strong electron-cyclotron maser is found in the presence of a magnetic-field-aligned electric potential drop which has several effects. For example, it can dilute the local plasma to such an extent that the plasma enters the regime in which the electron-cyclotron maser becomes effective and favours emission in a direction roughly perpendicular to the ambient magnetic field. This emission is the most intense, since it implies the coherent resonant contribution of a maximum number of electrons in the distribution function. What is more, such an instability can be sustained over a range of heights above the stellar surface, thus producing pseudo broadband, coherent radio emission, which would explain the simultaneous detection of both 8.4 and 4.9 GHz emission from TVLM 513 (Hallinan et al. 2006, 2007) and

2MASS0036+18 (Berger et al. 2002, 2005). These conditions are fulfilled in the low density, high magnetic field strength regions over the poles of a large scale magnetic field.

The striking similarities in the emission of TVLM 513 and now 2MASS0746+20, in particular the highly polarized pulse, strongly suggest that 2MASS0746+20 is an analog of TVLM 513, i.e. another UCD producing electron cyclotron emission. Since we do not resolve the system, we cannot say which component is responsible for the observed emission. Yet, as in the cases of TVLM 513, the emission during the burst most likely comes from an active region with a size much smaller than the radius of the dwarf.

ECM emission is emitted at the electron cyclotron frequency ν_c and its harmonics, i.e. $\nu_c \approx 2.8 \times 10^6 B \text{ Hz}$. This gives maximum magnetic field strength $B_{\text{max}} \approx 1.75 \text{ kG}$ for 2MASS 0746+20 as compared to $B_{\text{max}} \approx 3 \text{ kG}$ derived for TVLM 513. Reiners & Basri (2007) recently suggested the presence of magnetic fields of such strength on late M dwarfs via direct measurements, although these were filling factor dependent. Of the fourteen dwarfs of spectral type M5.0 or later, all but four show the presence of magnetic fields stronger than 1 kG.

Further high sensitivity radio observations of 2MASS0746+20 are needed, in particular a longer time series. Resolving the system to its components will identify the component responsible for the radio emission. It is also possible that both components are pulsing in which case, using Fourier analysis techniques, one may be able to extract the period of rotation of both dwarfs and determine the inclination angle of the equatorial plane to the orbital plane, using previously determined $\nu \sin i$.

6. Conclusions

The fraction of UCDs with detected radio emission so far is $\approx 10\%$ (Berger 2006, Phan-Bao et al. 2006). Yet, recent observations give us reason to think that this value may be underestimated. The above figure is based on VLA surveys at 8.5 GHz and with the assumption that the emission from these objects is stable over long periods of time. However, in the context of the electron cyclotron maser, emission at 8.5 GHz would require the presence of magnetic fields strengths up to $\approx 3 \text{ kG}$. Thus any objects with weaker fields would be undetected at that frequency, as is the case of 2MASS0746+20. On the other hand, recent VLA observations of the L2.5 brown dwarf 2MASS J05233822-1403022 reveal the possibility that levels of ECM emission generated in UCDs can vary significantly over months (Antonova et al. 2007).

Taking into account the above considerations, it is clear that despite the progress made in understanding the production mechanism of radio emission from ultracool dwarfs, the actual fraction of dwarfs, capable of producing radio emission, as well as the fraction of those, that show periodic pulsations is still unclear. The detection of emission at 4.9 GHz from 2MASS0746+20 points strongly towards the electron cyclotron maser instability as a more likely emission mechanism, at least for the short duration pulse. However, further followup observations are required.

Acknowledgements. Armagh Observatory is grant-aided by the N. Ireland Dept. of Culture, Arts & Leisure. We gratefully acknowledge the support of Science Foundation Ireland (Grant Number 07/RFP/PHYF553). This research has made use of the Simbad database, operated at CDS, Strasbourg, France.

References

- Audard, M., Osten, R. A., Brown, A., Briggs, K. R., Güdel, M., Hodges-Kluck, E. & Gizis, J. E., 2007 A&A 471, 63

- Bailer-Jones, C.A.L. & Mundt, R., 2001, *A&A* 374, 1071
Bailer-Jones, C. A. L., 2004 *A&A*, 419, 703
Berger, E., et al. 2001, *Nat* 410, 338
Berger, E., 2002, *ApJ* 572, 503
Berger, E., et al. 2005, *ApJ* 627, 960
Berger, E., 2006, *ApJ* 648, 629
Bouy, H., et al. 2004, *A&A* 423, 341
Burgasser, A.J. & Putman, M.E., 2005, *ApJ* 626, 486
Clarke, F. J., Oppenheimer, B. R. & Tinney, C. G., 2002, *MNRAS* 335, 1158
Dahn, C. C., et al. 2002, *AJ* 124, 1170
Donati, J. F., et al. 2007, *astro.ph.*2159
Ergun, R. E., Carlson, C. W., McFadden, J. P., Delory, G. T., Strangeway, R. J. & Pritchett, P. L., 2000, *ApJ* 538, 456
Gizis, J. E., Monet, D. G., Reid, I. N., Kirkpatrick, J. D., Liebert, J. & Williams, R. J., 2000, *AJ* 120, 1085
Gizis, J. E., Reid, I. N., Knapp, G. R., Liebert, J., Kirkpatrick, J. D., Koerner, D. W. & Burgasser, A. J., 2003, *AJ* 125, 3302
Gizis, J. E. & Reid, I. N., 2006, *AJ* 131, 638
Golimowski, D. A., Leggett, S. K., Marley, M. S., Fan, X., Geballe, T. R., Knapp, G. R., Vrba, F. J., Henden, A. A., Luginbuhl, C. B., Guetter, H. H., Munn, J. A., Canzian, B., Zheng, W., Tsvetanov, Z. I., Chiu, K., Glazebrook, K., Hoversten, E. A., Schneider, D. P. & Brinkmann, J., 2004, *AJ* 127, 3516
Hallinan, G., Antonova, A., Doyle, J.G., Bourke, S., Briskeen, W.F. & Golden, A., 2006, *ApJ* 653, 690
Hallinan, G., Lane, C., Bourke, S., Antonova, A., Doyle, J.G., Zavala, R.T., Briskeen, W.F., Boyle, R.P., Vrba, F.J. & Golden, A., 2007a, *ApJ* 663, L25
Kirkpatrick, J. D., Beichman, C. A. & Skrutskie, M. F. 1997, *ApJ* 476, 311
Kirkpatrick, J. D., Reid, I. N., Liebert, J., Cutri, R. M., Nelson, B., Beichman, C. A., Dahn, C. C., Monet, D. G., Gizis, J. E. & Skrutskie, M. F., 1999, *ApJ*, 519, 802
Kirkpatrick, J. D., Reid, I. N., Liebert, J., Gizis, J. E., Burgasser, A. J., Monet, D. G., Dahn, C. C., Nelson, B. & Williams, R. J., 2000, *AJ* 120, 447
Knapp, G. R., et al. 2004, *AJ* 127, 3553
Lane, C., Hallinan, G., Zavala, R.T., Butler, R.F., Boyle, R.P., Bourke, S., Antonova, A., Doyle, J.G., Vrba, F.J. & Golden, A., 2007, *ApJ* 668, L163
Leggett, S.K., et al. 2002, *ApJ* 564, 452
Liu, M. C. & Leggett, S. K., 2005 *ApJ*, 634, 616
Mohanty, S. & Basri, G., 2003 *ApJ*, 583, 451
Neuhäuser, R., Briceño, C., Comerón, F., Hearty, T., Martín, E. L., Schmitt, J. H. M. M., Stelzer, B., Supper, R., Voges, W. & Zinnecker, H., 1999 *A&A* 343, 883
Osten, R.A., Hawley, S.L., Bastian, T.S. & Reid, I.N., 2006, *ApJ* 637, 518
Phan-Bao, N., Osten, R.A., Lim, J., Martin, E.L. & Ho, P.T.P., 2007 *ApJ* 658, 553
Reid, I. N., Kirkpatrick, J. D., Gizis, J. E., Dahn, C. C., Monet, D. G., Williams, R. J., Liebert, J. & Burgasser, A. J., 2000, *AJ* 119, 369
Reid, I. N., Gizis, J. E., Kirkpatrick, J. D. & Koerner, D. W., 2001 *AJ*, 121, 489
Reid, I. N., Kirkpatrick, J. D., Liebert, J., Gizis, J. E., Dahn, C. C. & Monet, D. G., 2002 *AJ*, 124, 519
Reiners, A. & Basri, G., 2007, *ApJ* 656, 1121
Ruiz, M. T., Leggett, S. K. & Allard, F., 1997 *ApJ* 491, L107
Strauss, M. A., et al. 1999, *ApJ* 522L, 61
Treuemann, R.A., 2006, *A&A Rv* 13, 229
Vrba, F. J., et al. 2004, *AJ* 127, 2948
Zarka, P., 1998 *JGR* 103, 20159